ACS APPLIED MATERIALS & INTERFACES

www.acsami.org

Research Article

A Wireless, CRISPR-Polymer Dot Electrochemical Sensor for the Diagnosis of Bacterial Pneumonia and Multi-Drug Resistance

San Hae Im,[#] Akhmad Irhas Robby,[#] Heewon Choi, Ju Yeon Chung, Yang Soo Kim,[*] Sung Young Park,[*] and Hyun Jung Chung[*]

Cite This: *ACS Appl. Mater. Interfaces* 2024, 16, 5637−5647

Read Online

ACCESS | Metrics & More | Article Recommendations | Supporting Information

ABSTRACT: Rapid and accurate diagnosis is crucial for managing the global health threat posed by multidrug-resistant bacterial infections; however, current methods have limitations in either being time-consuming, labor-intensive, or requiring instruments with high costs. Addressing these challenges, we introduce a wireless electrochemical sensor integrating the CRISPR/Cas system with electroconductive polymer dot (PD) nanoparticles to rapidly detect bacterial pathogens from human sputum. To enhance the electroconductive properties, we synthesized copper-ion-immobilized PD (PD-Cu), followed by conjugation of the deactivated Cas9 protein (dCas9) onto PD-Cu-coated Si electrodes to generate the dCas9-PD-Cu sensor. The dCas9-PD-Cu sensor integrated with isothermal amplification can specifically detect target nucleic acids of multidrug-resistant bacteria, such as the antibiotic resistance genes *kpc-2* and *mecA*. The dCas9-PD-Cu sensor exhibits high sensitivity, allowing for the detection of ∼54 femtograms of target nucleic acids, based on measuring the changes in resistivity of the Si electrodes through target capture by dCas9. Furthermore, a wireless sensing platform of the dCas9-PD-Cu sensor was established using a Bluetooth module and a microcontroller unit for detection using a smartphone. We demonstrate the feasibility of the platform in diagnosing multidrug-resistant bacterial pneumonia in patients' sputum samples, achieving 92% accuracy. The current study presents a versatile biosensor platform that can overcome the limitations of conventional diagnostics in the clinic.

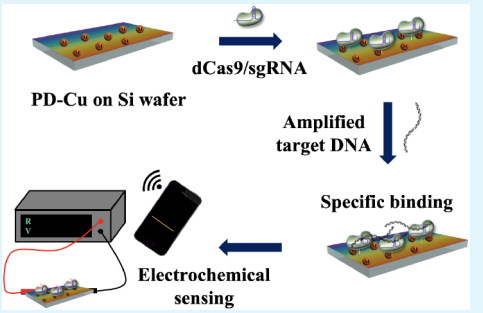

KEYWORDS: *CRISPR/Cas, polymer dot, electrochemical detection, wireless sensing, bacterial pneumonia, multidrug resistance*

INTRODUCTION

Bacterial infections have been a major threat to global health, accounting for 13.6% of deaths worldwide.[1−3] Particularly, the emergence and spread of multidrug-resistant bacteria have become a major problem[4] and are predicted to cause 10 million deaths annually by the year 2050.[5] To prevent the spread of the disease, rapid and accurate diagnosis is crucial; however, diagnosis in the clinic relies on microbial culture which is time-consuming.[6] Molecular diagnostic techniques based on immunoassays are rapid and affordable as point-of-care tests but lack sensitivity and require the development of specific antibodies. On the contrary, genetic detection can be versatilely applied to various molecular targets and exhibits high sensitivity. However, standard quantitative real-time PCR (qPCR) involves complex sample processing requiring trained personnel.[7−10] Integrated systems such as the BioFire FilmArray and GeneXpert have been developed but show limited applicability due to the high instrumental cost.

The clustered regularly interspaced short palindromic repeats (CRISPR) system, which can precisely correct the genomes of cells, offers a promising approach for diagnosis due to the high selectivity.[11−20] Diagnostic platforms based on the CRISPR system include the DNA Endonuclease-Targeted CRISPR Trans Reporter (DETECTOR)[21] and Specific High Sensitivity Enzymatic Reporter UnLOCKING (SHERLOCK),[22,23] that are based on the collateral cleavage by Cas12a and Cas13a, respectively. Although these platforms exhibit remarkable sensitivity, limitations remain due to the chance of false-positives in optical detection methods. Deactivated Cas9 (dCas9), which can bind to nucleic acid targets with high selectivity without inducing cleavage, lack the sensitivity for applications in molecular diagnosis.[24−30]

Electrochemical sensors can provide a versatile diagnostic platform for various disease targets due to the high sensitivity and reliability.[31] However, the previous methods have used materials with poor water solubility and limited modification capabilities.[32−37] Polymer dot nanoparticles (PDs) have been developed as an alternative to semiconductor quantum dots (SQDs) to overcome the toxicity associated with heavy metals.[38] PDs exhibit excellent water solubility and electroconductivity, rendering them great advantages as sensing

Received: November 15, 2023
Revised: January 8, 2024
Accepted: January 11, 2024
Published: January 26, 2024

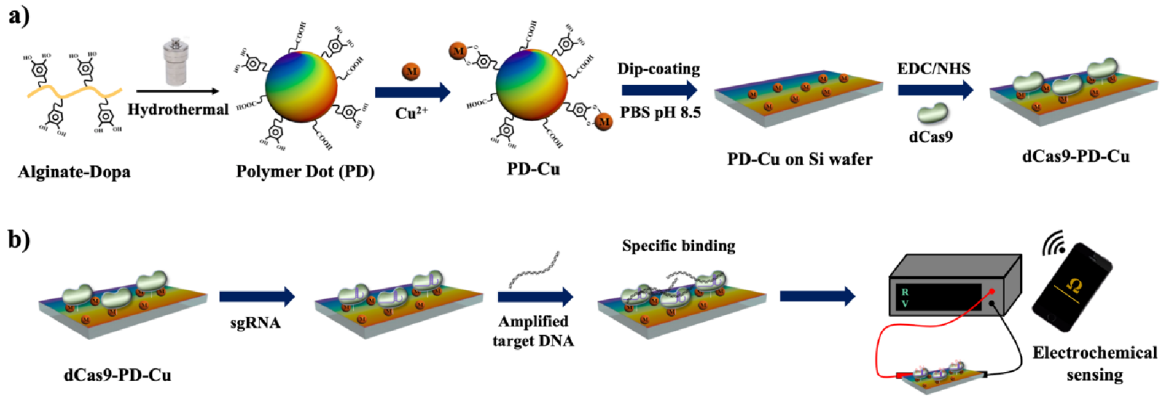

Figure 1. Schematic of the dCas9-PD-Cu sensor. (a) Fabrication of the sensor comprising hydrothermally synthesized PDs, immobilized with Cu^{2+} and coated on the Si wafer followed by conjugation of dCas9. (b) Electrochemical detection of target DNA by dCas9-PD-Cu complexed with a specific sgRNA, followed by sourcemeter measurement or wireless sensing.

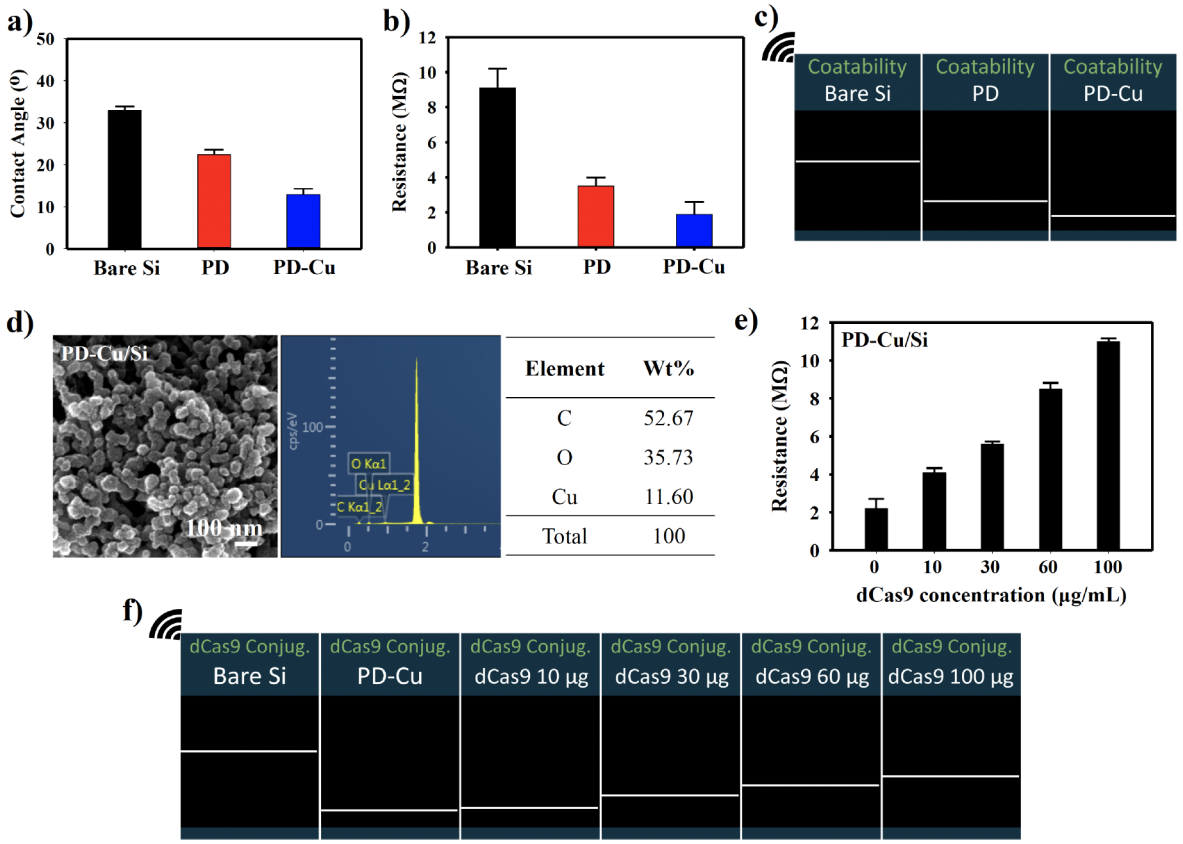

Figure 2. Preparation and characterization of the dCas9-PD-Cu sensor. (a) Static contact angle and (b,c) resistance measurements by (b) sourcemeter and (c) wireless detection of bare, PD-coated and PD-Cu-coated Si wafer. (d) SEM-EDX analysis of PD-Cu-coated Si wafer. Scale bar 100 nm. (e-f) Resistance measurements of dCas9-conjugated PD-Cu-coated Si wafer at various concentrations of dCas9 (0−100 μg/mL), by (e) sourcemeter and (f) wireless detection.

materials.[39−41] Moreover, PDs can be endowed with diverse functions via surface modification, such as stimuli responsiveness, adhesion to targets, or selective binding of analytes.[39]

Here, we introduce a robust and sensitive platform using the CRISPR/Cas system functionalized onto PD electrochemical sensors for the diagnosis of multidrug-resistant bacterial pneumonia (Figure 1). We hypothesized that using the highly specific CRISPR/Cas detection based on dCas9, and PD which exhibits high electroconductivity, can provide a versatile and rapid diagnostic platform with high sensitivity. A dCas9-conjugated copper ion-immobilized PD sensor (dCas9-PD-Cu) is developed and demonstrated to rapidly detect bacterial gene targets in the presence of a specific single-guide RNA, such as the antibiotic resistance gene *kpc-2* from carbapenem-resistant *Klebsiella pneumoniae* (CRKP), and *mecA* from methicillin-resistant *Staphylococcus aureus* (MRSA). Furthermore, we established a wireless sensing platform using the dCas9-PD-Cu sensor integrated with isothermal amplification to achieve high sensitivity and specificity. We validate the clinical applicability of the sensor to diagnose multidrug-resistant bacterial pneumonia in patients' sputum samples. The current platform can be potentially applied for rapid

https://doi.org/10.1021/acsami.3c17151
ACS Appl. Mater. Interfaces 2024, 16, 5637−5647

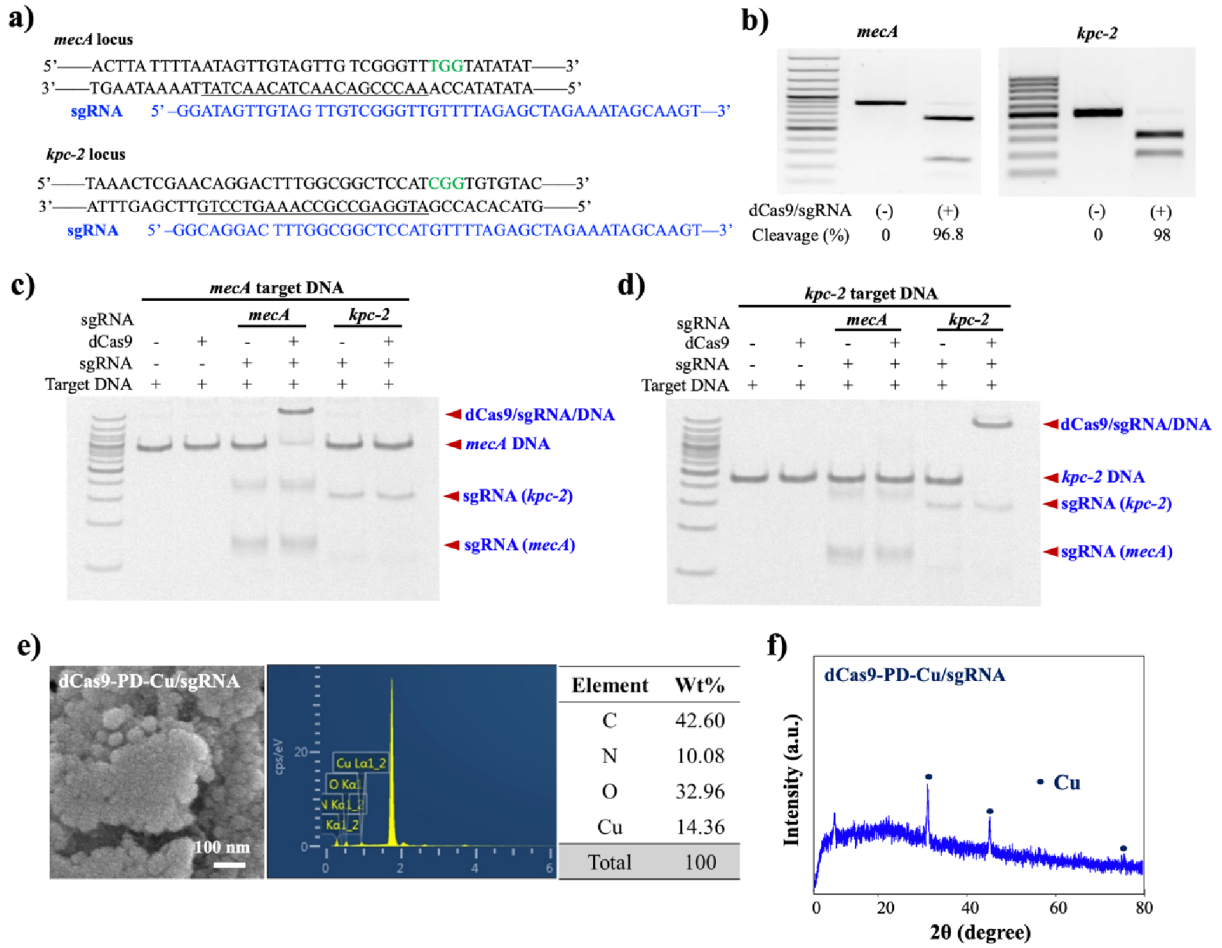

Figure 3. Functional characterization of dCas9-PD-Cu with sgRNA. (a) Scheme of specific sgRNA sequences for *mecA* and *kpc-2* aligned with the target DNA sequences. (b) Specificity of sgRNAs targeting *mecA* and *kpc-2* when complexed with Cas9, treated to the corresponding target DNAs, and analyses of cleaved products. (c,d) Binding specificity of sgRNAs complexed with dCas9 toward each target DNA determined by gel retardation for (c) *mecA* and (d) *kpc-2* genes. (e) SEM-EDX and (f) XRD profiles of dCas9-PD-Cu complexed with sgRNA. Scale bar 100 nm.

diagnostics at the bedside by overcoming the limitations of conventional methods used in the clinic.

RESULTS AND DISCUSSION

Fabrication and Characterization of dCas9-PD-Cu. Copper ion-immobilized PD (PD-Cu)-coated electrodes were prepared as the substrate for modification with dCas9 and electrochemical detection of target DNA. To specifically detect the DNA of multidrug-resistant bacteria, the modified dCas9-PD-Cu electrode was further functionalized with specific sgRNA, such as *mecA* sgRNA (for targeting *mecA*) and *kpc-2* sgRNA (for targeting *kpc-2*). During the process of detection, the target DNA will bind with electrode surface due to high affinity of sgRNA toward the target DNA. As the target DNA is a nonconductive organic compound, its attachment will significantly increase the resistivity of the electrode compared to the initial resistivity before detection. Based on this phenomenon, the change in electrode resistivity was used as the indication of the presence of target DNA in the sample, which could also be monitored via a wireless sensing device. PDs are known for their high versatility for chemical modification owing to the presence of various surface functional groups. In this case, dopamine that was conjugated on the PDs was utilized for immobilizing the Cu^{2+} ion onto the PD surface to enhance the electroconductivity and electron transfer, which is essential for electrochemical sensing. The presence of dopamine also provides adhesive properties to the PDs, allowing the nanoparticles to be easily coated on the surface of the electrode. Initially, the PD was synthesized via hydrothermal carbonization of alginate-dopa,[39] followed by reaction with Cu^{2+} to form PD-Cu. The optical properties of the as-synthesized PD-Cu were observed by using a UV−vis spectrometer and a photoluminescence (PL) spectrometer. Figure S1a shows the absorbance spectra of PD and PD-Cu, exhibiting absorbance peaks at 280 and 340 nm that are characteristics of the $\pi-\pi^*$ transition of dopamine. The PL spectra further showed that Cu^{2+} was effectively immobilized onto the PDs, reflected from the significant quenching of fluorescence for PD-Cu compared to PD (Figure S1b). The quenching of fluorescence for PD-Cu occurred by the photoinduced electron transfer (PET) mechanism between Cu^{2+} and PD.[42] The successful immobilization of Cu^{2+} could also be observed by the increase in particle size for PD-Cu (336 nm) compared to that for PD (233 nm) (Figure S1c). For fabrication of the sensor, the synthesized PD-Cu was coated on Si wafer using a dip-coating method. The formation of the PD-Cu coating on the Si wafer was determined using static contact angle measurements, using Bare Si and PD-coated Si wafer as controls. Contact angle measurements showed a decrease in the value from 32.9° (Bare Si) to 22.4°

https://doi.org/10.1021/acsami.3c17151
ACS Appl. Mater. Interfaces 2024, 16, 5637−5647

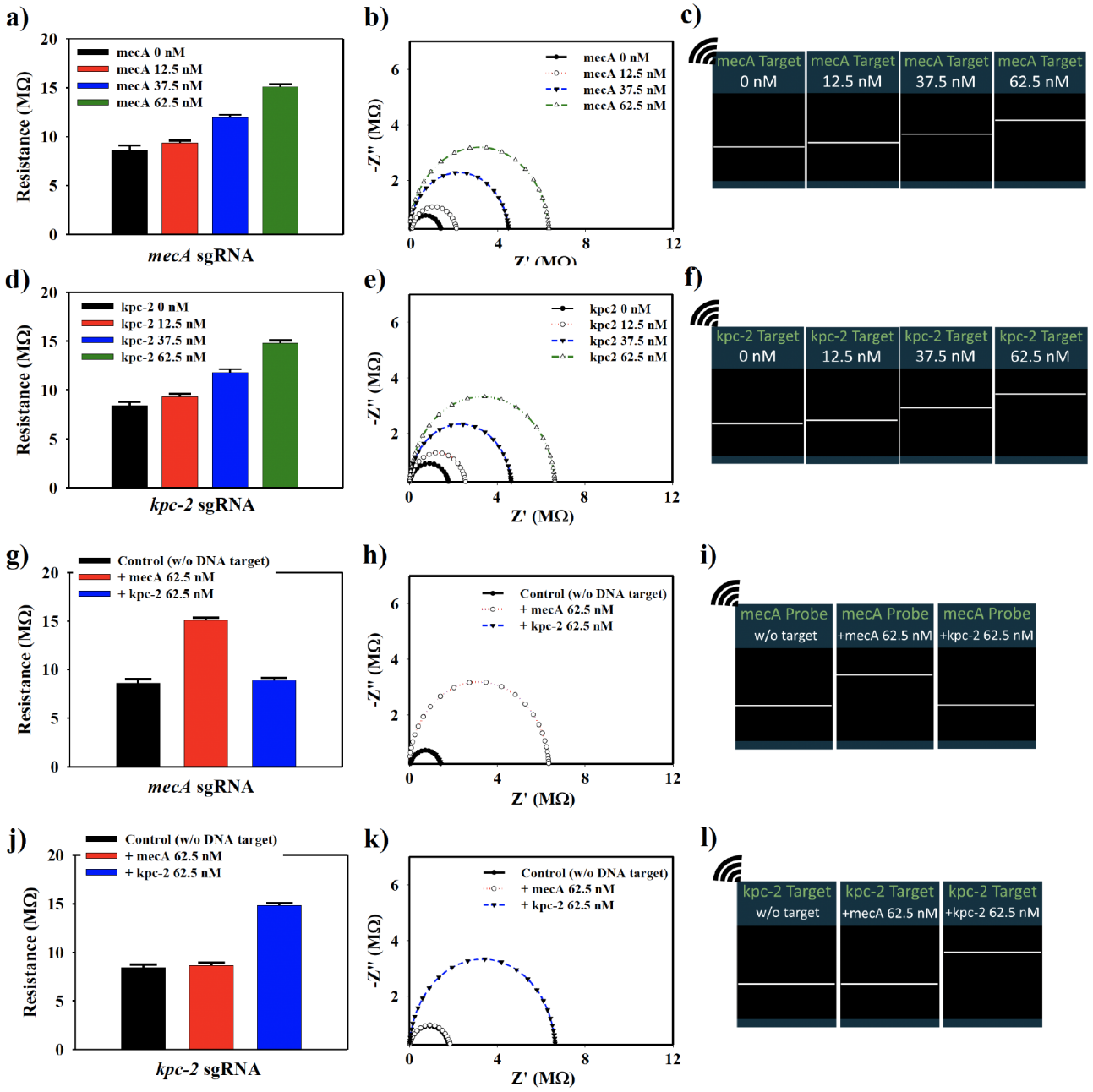

Figure 4. Electrochemical sensing of target DNA with dCas9-PD-Cu. (a–f) Detection of target DNAs at various concentrations (0–62.5 nM) by (a,d) sourcemeter, (b,e) EIS, and (c,f) wireless sensing. Target DNAs were detected using the corresponding sgRNAs for target genes (a–c) *mecA* and (d–f) *kpc-2*. (g–l) Determination of cross-reactivity of the sgRNAs with dCas9-PD-Cu by (g,j) sourcemeter, (h,k) EIS, and (i,l) wireless sensing for target DNAs and the corresponding sgRNAs for (g–i) *mecA* and (j–l) *kpc-2* genes (target DNA concentration: 62.5 nM).

after coating with PD, while coating with PD-Cu showed a further decrease to 12.9° due to the increased hydrophilicity (Figure 2a). When the contact angles of PD and PD-Cu-coated Si wafers were compared, the results revealed that PD-Cu was more hydrophilic than PD owing to the presence of the Cu^{2+} ion. Furthermore, the measurement of resistance using a sourcemeter showed a decrease in values from 9.1 MΩ (Bare Si) to 3.7 MΩ after coating with PD and to 2.2 MΩ after coating with PD-Cu (Figure 2b). The decrease in resistance, particularly for the PD-Cu-coated Si wafer, reveals that the attachment of PD and Cu^{2+} improved the conductivity of the surface due to the presence of the $\pi-\pi^*$ bond in PD and the ionic conductivity of Cu^{2+}. Wireless detection of the PD and PD-Cu-coated surfaces using a microcontroller (Arduino Uno) and a Bluetooth module (AppGosu) showed similar changes in resistance values, as shown in the sourcemeter measurements (Figure 2c). The coatability of PD-Cu was also assessed on a PET substrate, showing a similar pattern when compared to coating on the Si wafer, with PD-Cu exhibiting the lowest contact angle and resistance values compared to Bare PET and PD-coated PET (Figure S2a,b). Scanning electron microscopy-energy dispersive X-ray spectroscopy (SEM-EDX) further confirmed the coating of PD-Cu nanoparticles on the Si wafer, with the detection of C (52.67%), O (35.73%), and Cu (11.60%) that corresponded to PD-Cu (Figure 2d). The fabricated PD-Cu-coated Si wafer was then conjugated with

https://doi.org/10.1021/acsami.3c17151
ACS Appl. Mater. Interfaces 2024, 16, 5637–5647

FPLC-purified dCas9 (Figure S3) in various concentrations (10, 30, 60, and 100 μg/mL) via the EDC-NHS reaction. The gradual increase in resistance when conjugated at higher dCas9 concentrations was confirmed by sourcemeter measurements (Figure 2e), as well as by wireless sensing (Figure 2f). The results demonstrate the successful preparation of the dCas9-PD-Cu sensor for wireless electrochemical detection.

sgRNA Design and Complexation with dCas9-PD-Cu. sgRNAs were designed to include 20 nt sequences specific for the *mecA*, *kpc-2*, *NDM-1*, and *ClfA* genes (Figure 3a and Table S1). Target sequences were selected considering the theoretical off-target number and synthesized by *in vitro* transcription (Figure S4). sgRNAs were characterized by measuring cleavage activity and gel retardation. Among the designed sgRNAs, sgRNA 5 targeting *mecA* and sgRNA 3 targeting *kpc-2* showed 96.8%, and 98.0% cleavage efficiencies, respectively (Figures 3b and S5), while sgRNA 5 targeting *NDM-1*, and sgRNA 3 targeting *ClfA* resulted in 96.4% and 94.5%, respectively (Figure S6). The selected sgRNAs were able to efficiently bind to the target DNA in the presence of dCas9 (Figures 3c,d, and S7). The selected sgRNAs were used for further experiments.

Next, we allowed the sgRNAs to complex with dCas9-PD-Cu by incubating with an excess amount of sgRNA. The SEM-EDX data reveal that the dCas9/sgRNA ribonucleoprotein complexes were efficiently conjugated onto the surface of the PD-Cu-coated Si wafer, indicated by the presence of nitrogen (N) on the surface at approximately 10.08% (Figure 3e). These results reconfirm the successful conjugation of dCas9 and sgRNA onto the PD-Cu-coated Si wafer. XRD analysis showed a broad diffraction peak at 8°−25° corresponding to the graphitic carbon of PD, and diffraction peaks at 31°, 45°, and 75° corresponding to the presence of Cu on the surface (Figure 3f). By the electrochemical property of PD-Cu on the Si wafer, resistance measurements with the sourcemeter showed an increase from 6.31 to 8.61 MΩ upon complexation of dCas9 with *mecA* sgRNA, and to 8.42 MΩ with *kpc-2* sgRNA (Figure S8). The increase in resistance can be due to the presence of an organic compound (sgRNA) on the surface of the Si wafer. This confirmed the successful complexation of sgRNA with dCas9 on the sensor that would endow specificity of detection to each genetic target. Since dCas9 conjugation also resulted in a significant increase in the resistance of PD-Cu, setting the baseline for detection would be important for sensitive detection of the target.

Electrochemical Sensing by dCas9-PD-Cu. We attempted to detect target DNA by specific binding with sgRNA complexed with dCas9-PD-Cu by electrochemical sensing. We added synthetic target DNA at various concentrations to dCas9-PD-Cu/sgRNA to determine the sensitivity of the method. To exclude interfering signals from residual salts, we performed measurements for control samples without target DNA (= 0 nM). As the concentration of *mecA* target DNA added to the dCas9-PD-Cu with *mecA* sgRNA was increased from 0 nM to 12.5, 37.5, and 62.5 nM, the resistance values measured by the sourcemeter gradually increased from 8.61 MΩ to 9.34, 11.95, and 15.09 MΩ (Figure 4a). The increase in the resistance at higher *mecA* DNA concentrations confirms that the target DNA was captured on the surface of the dCas9-PD-Cu sensor. Electrochemical impedance spectroscopy (EIS) also revealed that the dCas9-PD-Cu sensor could detect *mecA* target DNA, indicated by the increase in impedance depending on the *mecA* concentration (Figure 4b). Moreover, wireless sensing also demonstrated the resistance changes according to *mecA* concentrations, similar to the results obtained from the sourcemeter and EIS (Figure 4c). We also evaluated the sensor toward another type of target DNA (*kpc-2*) by modifying the dCas9-PD-Cu sensor with sgRNA for *kpc-2*. A similar trend was observed for detecting *kpc-2* target DNA using dCas9-PD-Cu by the sourcemeter, EIS, and wireless sensing measurements, with resistance values changing from 8.42 MΩ (0 nM) to 9.31 MΩ (12.5 nM), 11.77 MΩ (37.5 nM), and 14.81 MΩ (62.5 nM) (Figure 4d−f). These results reveal that electrochemical sensing using dCas9-PD-Cu is feasible for target DNA detection by employing a specific type of sgRNA, exhibiting a concentration-dependent manner, and is able to detect low concentrations of DNA. Furthermore, the signals by wireless sensing also demonstrate that the dCas9-PD-Cu sensor is highly robust, which is a critical requirement for applications in diagnostics. The cross-reactivity between the electrode and a nonspecific target was also examined by treating the dCas9-PD-Cu/sgRNA (*kpc-2*) electrode with *mecA* synthetic target DNA. The electrochemical measurements (EIS, sourcemeter, and wireless sensor) shown in Figure S9 revealed that the resistance value was unchanged toward the nonspecific target, confirming that the dCas9-PD-Cu electrode can only detect a specific target DNA depending on the type of conjugated sgRNA on the electrode surface.

The specificity of the dCas9-PD-Cu sensor was further assessed by examining cross-reactivity of the sgRNA probes with nontarget DNA as the controls. For sensing using the *mecA* sgRNA probe, the resistance value was 15.09 MΩ when the probe was added with *mecA* target DNA, which was significantly higher than when the probe was added with *kpc-2* target DNA (8.89 MΩ) as the control (Figure 4g). These results were also observed from the EIS measurements as well as wireless sensing (Figure 4h,i). Sensing based on the *kpc-2* sgRNA probe also gave rise to resistance changes when added with *kpc-2* target DNA (14.81 MΩ) according to the sourcemeter, EIS, and wireless sensing (Figure 4j−l). On the contrary, the *mecA* target DNA did not result in significant changes in resistance (8.68 MΩ), resulting in values that were almost the same as before binding with the *kpc-2* sgRNA probe (8.42 MΩ). These results demonstrate the high specificity of detecting target DNA when using the dCas9-PD-Cu sensor in the presence of sgRNA.

Validation of dCas9-PD-Cu with Cultured Bacteria. To demonstrate that the dCas9-PD-Cu sensor can be used for the diagnosis of biological samples, we attempted the detection of nucleic acids derived from cultured bacteria. The direct detection of target RNA within a bulk solution of total RNA is extremely challenging due to the small portion of target RNA and the interference by nontarget RNAs.[43] Therefore, we integrated loop-mediated amplification (LAMP), which can increase the copy number of target RNA in solution at isothermal conditions, to make diagnosis feasible at the bedside. A one-pot reaction of reverse transcription (RT) and LAMP was performed prior to sensing with dCas9-PD-Cu. We designed LAMP primers for three different target regions for each target gene, to select the one with the highest specificity against five bacterial strains (*E. coli*, *Pseudomonas aeruginosa*, CRKP, MSSA, and MRSA). Characterization of the LAMP products enabled the selection of primers with the highest specificity for target genes *mecA*, *kpc-2*, *NDM-1*, and *ClfA* (Figure S10). To establish the optimal conditions for LAMP, we attempted the reaction for 5, 10, 30, and 60 min. A

https://doi.org/10.1021/acsami.3c17151
ACS Appl. Mater. Interfaces 2024, 16, 5637−5647

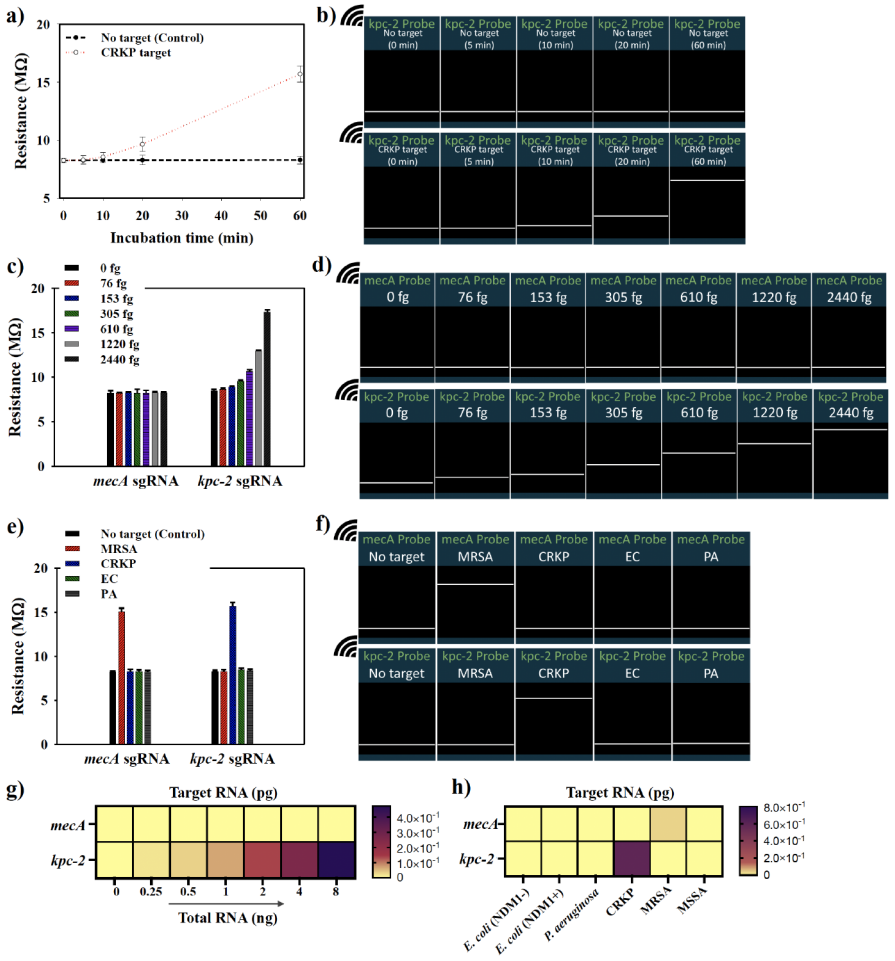

Figure 5. Validation of dCas9-PD-Cu in cultured bacteria. Electrochemical sensing of target RNA from cultured bacteria after RT and LAMP, according to (a,b) various incubation times (0−60 min) for LAMP (CRKP target; *kpc-2* sgRNA), (c,d) various target RNA concentrations from CRKP (0−2440 fg; *kpc-2* sgRNA), and (e,f) various bacterial targets (*kpc-2* sgRNA; CRKP compared with MRSA, EC (*E. coli*), and PA (*P. aeruginosa*) as controls), using (a,c,e) sourcemeter and (b,d,f) wireless sensing. (g,h) Detection of target genes by qPCR according to (g) total RNA amount (*kpc-2* target RNA; 0−8 ng), and (h) bacterial strains.

reaction time of 30 min resulted in the multiple bands like a ladder, which are the general characteristic of LAMP products upon gel electrophoresis.[44] When the reaction time was extended to 60 min, the multiple band patterns appeared as well; however, nonspecific bands also appeared for the negative control sample that did not include bacteria (Figure S11). Therefore, a reaction time of 30 min was selected for amplification in the following experiments.

We then carried out sensing of bacterial RNA samples using dCas9-PD-Cu integrated with LAMP. We tried detecting the amplified products derived from CRKP total RNA with dCas9-PD-Cu complexed with *kpc-2* sgRNA at various incubation times. As the incubation time increased from 0 to 60 min, the resistance values gradually increased from 8.25 to 15.7 MΩ (Figure 5a). Wireless sensing showed patterns similar to those of the sourcemeter measurements, with proportional increases in signals as the incubation time was increased (Figure 5b). Significant changes in resistance values were observed from 20 min incubation, determining that 20 min was sufficient for wireless detection. Since longer incubation times resulted in higher signals, the conditions can be adjusted depending on the sensitivity required for various targets.

We evaluated the sensitivity of dCas9-PD-Cu by performing measurements with amplified products from various initial amounts of target RNA. We observed that increasing the target RNA amounts derived from CRKP from 75 to 2440 fg resulted in a gradual increase in resistance from 8.67 to 17.32 MΩ for the *kpc-2* probe (Figure 5c). On the contrary, addition of amplified products from CRKP RNA did not result in any signal changes for the *mecA* sgRNA probe, demonstrating the specificity of detection. The limit of detection (LOD) with the PD-Cu-dCas9 sensor was estimated to be 54 fg of target RNA, demonstrating that the sensitivity was 10-fold higher compared to LAMP alone based on sourcemeter measurements (Figure S12). Wireless sensing also showed the typical changes in conductivity that could be visualized from target RNA amounts of 75 fg, confirming the high sensitivity of the method (Figure 5d).

We next validated the specificity of dCas9-PD-Cu sensing by testing with samples derived from various bacterial strains. Sourcemeter measurements showed that only the target RNA derived from MRSA, the strain that expresses *mecA*, resulted in a significant increase in resistance for dCas9-PD-Cu complexed with the *mecA* sgRNA, while the controls CRKP, *E. coli*, and *P. aeruginosa* did not (Figure 5e). Similarly, the *kpc-2* sgRNA only gave rise to significant changes for CRKP, while changes were not observed for the nontarget controls. These results were obviously shown from the wireless sensing results, as well

https://doi.org/10.1021/acsami.3c17151
ACS Appl. Mater. Interfaces 2024, 16, 5637−5647

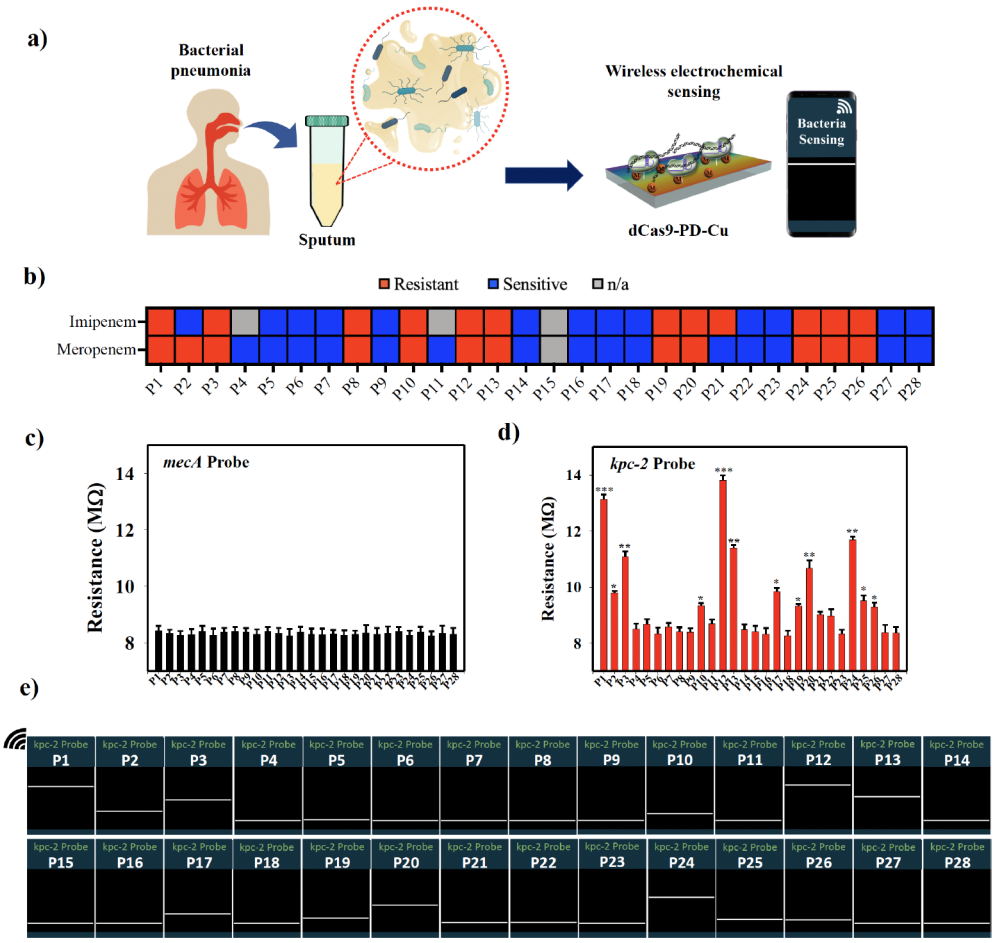

Figure 6. Diagnosis of bacterial pneumonia in patients' sputum. (a) Schematic illustration of sensing with dCas9-PD-Cu. (b) Microbial culture results on susceptibility of bacteria detected in the patients' samples (no. 1−28). (c,d) dCas9-PD-Cu sensing results using (c) *mecA* sgRNA and (d) *kpc-2* sgRNA with the sourcemeter (*$p < 0.05$, **$p < 0.01$, ***$p < 0.001$). (e) Wireless sensing results of dCas9-PD-Cu with *kpc-2* sgRNA.

(Figure 5f). To verify our results from dCas9-PD-Cu with a gold standard method, qPCR was performed for the equivalent RNA samples. Figure 5g shows that the concentration-dependent increases in signals appeared, which was comparable to the dCas9-PD-Cu sensing results. The cross-reactivity of the target RNAs derived from the different bacterial strains also appeared low, according to the qPCR results (Figures 5h and S13). One note is that a relatively low signal was observed from qPCR for *mecA* for the MRSA sample. Considering the substantial changes in resistance values for dCas9-PD-Cu even at the level of tens of femtograms, these results suggest the possible advantage of the current technology in providing a more robust and sensitive platform. dCas9-PD-Cu has an LOD value that is approximately 180 times higher than that of the commercially available BioFire FilmArray (LOD: $10^{3.5}$ copies/mL) which is based on multiplex PCR. However, the dCas9-PD-Cu (1 × 1, L × W, cm) uses a smaller instrument, a sourcemeter (20 × 40 × 10, L × W × H, cm), compared to the BioFire FilmArray (39.3 × 16.5 × 45.8, L × W × H, cm), and is also half the price. Additionally, dCas9-PD-Cu can provide diagnostic results within 1 h with reagents that cost less than $15 per test. Therefore, we believe that the dCas9-PD-Cu sensor can be a cost-effective diagnostic platform for rapid bedside diagnosis compared with the previously commercialized platforms.

Diagnosis of Bacterial Pneumonia in Sputum. For evaluation as a diagnostic platform in the clinic, dCas9-PD-Cu was applied to sputum samples obtained from patients with bacterial pneumonia. Sputum samples were collected from a total of 28 patients and processed to obtain total RNA, followed by RT and LAMP for detection with dCas9-PD-Cu (Figure 6a). Microbial culture performed in the clinical laboratory had identified the bacterial pathogen and the type of resistance against antibiotics such as carbapenem (Figure 6b). Among the 28 sputum samples, resistance to either imipenem or Meropenem was detected in 13 samples, and among these, 11 samples were resistant to both carbapenems. Bacterial pathogens included *K. pneumoniae* in 4 samples, *P. aeruginosa* in 5 samples, and Acinetobacter species in 5 samples. None of the samples were detected with Gram-positive bacteria, nor showed oxacillin resistance that is a characteristic of MRSA. Resistance measurements by the sourcemeter and wireless sensing using dCas9-PD-Cu with the *mecA* sgRNA showed only background levels, as can be expected since none of the samples were detected with MRSA (Figures 6c and S14). With the *kpc-2* sgRNA, surges in resistance values were shown for 12 of the samples, and could be determined as "positive" by dCas9-PD-Cu sensing (Figure 6d,e). Eleven out of 12 samples that were detected positive for *kpc-2* by dCas9-PD-Cu were also diagnosed with carbapenem resistance by microbial culture, resulting in a correlation of

https://doi.org/10.1021/acsami.3c17151
ACS Appl. Mater. Interfaces 2024, 16, 5637−5647

92%. However, 2 out of the 13 samples that were diagnosed "positive" for a Gram-negative pathogen with resistance by microbial culture were determined as "negative" by dCas9-PD-Cu sensing, which can either be due to a culture-negative pathogen or involve a different resistance gene. qPCR was performed for the *mecA* and *kpc-2* genes to compare with the results by dCas9-PD-Cu sensing. According to the qPCR results, a total of 17 samples were detected positive for *kpc-2*, and this included all 13 samples that were diagnosed with carbapenem resistance by a microbial culture (Figure S15). This confirms that *kpc-2* was the major gene related to carbapenem resistance in pneumonia patients. The four samples that were determined as positive by qPCR, but negative by microbial culture can be due to the nonspecific signals resulting in false-positives, or culture-negative bacteria. When comparing the dCas9-PD-Cu sensing results with the qPCR results, 11 out of 12 samples that were determined positive from dCas9-PD-Cu sensing were also determined positive by qPCR. In sum, these results demonstrate the high correlation of dCas9-PD-Cu, microbial culture, and qPCR, and dCas9-PD-Cu sensing can provide a robust diagnostic platform that can be potentially applied at the bedside. However, methods to verify the samples that did not show correlation with either one of the methods should be further explored.

CONCLUSION

A wireless sensing platform based on dCas9-PD-Cu was developed and demonstrated its feasibility for diagnosis of bacterial pneumonia. In the clinical laboratory, the diagnosis of bacterial infections still relies on microbial culture, and qPCR has not been generally applied. As a wireless sensing platform, with the requirement of technical components that are relatively simple (Bluetooth module, Arduino microcontroller, and smartphone), the current platform can be usefully applied as a bedside assay that allows clinical decision making for treatment of the infection. With the sensitivity of down to tens of femtograms of RNA, the dCas9-PD-Cu sensor presents a major breakthrough from the previous electrochemical sensing methods that can even replace the limitations of qPCR-based diagnostics. The establishment of the method as an automated platform for practical applications will require resolving the engineering issues in providing a robust and user-friendly platform. Improving the throughput and specification of the technique should be achieved to enable the detection of a large number of biomarkers as well as deliberate selection of the markers for each syndrome.

EXPERIMENTAL SECTION

Materials. Dopamine hydrochloride, alginic acid sodium salt (MW: 155 000 g/mol), *N*-hydroxysuccinimide (NHS), ethylcarbodiimide hydrochloride (EDC), and copper(II) chloride ($CuCl_2$) were purchased from Sigma-Aldrich. Phosphate-buffered saline (PBS; pH 7.4) was purchased from Bioneer Corp. Silicon (Si) wafer (P-type) was obtained from Silicon Technology Corporation.

Preparation and Characterization of dCas9-PD-Cu Sensor. PDs containing dopamine were synthesized via hydrothermal carbonization of alginate-dopamine (180 °C, 8 h) according to a previous report.[39] The obtained PD was mixed with 10 wt % of $CuCl_2$ in PBS pH 8.5 for 12 h at room temperature, continued by dialysis (MWCO: 1 kDa) against DDW for 24 h and freeze-dried.[42] The PD-Cu sensor was then prepared using a dip-coating method. The sensor substrate (Si wafer, 1 × 1 cm^2) was soaked in PD-Cu solution (2 mg/mL in PBS pH 8.5) for 12 h at room temperature and washed with water before dried in open air for further use. The surface of the PD-Cu-coated Si wafer was then activated using EDC (20 mg/mL) for 30 min, followed by NHS (30 mg/mL in PBS pH 7.4) for 2 h. After washing the surface with PBS 7.4, the activated surface was soaked again in dCas9 solution (10, 30, 60, and 100 μg in 0.5 mL of PBS pH 7.4 solution) for 6 h at room temperature, washed with PBS pH 7.4, and dried until further use. UV−vis spectra of PD-Cu were recorded by using an Optizen 2020UV spectrophotometer (Mecasys Co.). Particle size was measured by dynamic light scattering (DLS; Zetasizer Nano; Malvern Panalytical). Photoluminescence (PL) spectra were obtained using an L550B luminescence spectrometer (PerkinElmer). Water contact angles of the coated surface were measured using a DO3210 instrument (KRUSS Ltd.). X-ray diffraction (XRD) was measured using AXS ADVANCE D-8 (Bruker). Scanning electron microscopy-energy dispersive X-ray (FE-SEM) profiles were observed by using a JSM-6700F SEM (JEOL). Electrochemical analysis was performed using a sourcemeter (Keithley 2450) and an electrochemical impedance spectrometer (EIS; CS350; CorrTest Instruments). For wireless sensing, a microcontroller (Arduino Uno; ATmega328P Processor), a Bluetooth module (AppGosu), and a smartphone were used.

Purification of dCas9 Protein. Cas9 or dCas9 expression plasmid (Figure S3a) was transformed to *E. coli* Rosetta (DE)3 cells using the heat shock method. Luria−Bertani (LB, BD Difco) agar plates, including 100 μg/mL ampicillin (Thermo Scientific) were used to select transformed bacterial colonies. The transformed plasmid was confirmed by colony PCR. For protein expression, transformed cells were incubated in ampicillin containing (100 μg/mL) LB media until OD_{600} is 0.8. 0.5 mM amount of isopropyl β-D-1-thiogalactopyranoside (IPTG) was added for induction at 18 °C for 16 h with gentle agitation. Cell pellets were collected and lysed in lysis buffer (50 mM Na_2PO_4, 300 mM NaCl, 10 mM imidazole, 1% TritonX-100, 0.5 mM PMSF, 1 mM DTT, 1 mg/mL lysozyme, 16.7 U/mL benzonase, and pH 8.0). Sonicated lysates were cleared using centrifugation (13,000 *g*, 30 min) and filtered using a 0.2 μm syringe filter. His-trapTM HP (GE Healthcare) and HiLoad Superdex 200 26/600 (GE Healthcare) chromatography were performed using ÄKTAprime Plus (GE Healthcare). Protein was eluted with elution buffer (50 mM Na_2PO_4, 300 mM NaCl, 250 mM imidazole, 0.05% β-mercaptoethanol, and pH 8.0) and dialyzed against storage buffer (50 mM Tris-Cl, 200 mM KCl, 0.1 mM EDTA, 1 mM dithiothreitol (DTT), 0.5 mM PMSF, 20% glycerol, and pH 8.0) using a Slide-A-Lyzer dialysis device (MWCO: 20 kDa, Thermo Scientific).

sgRNA Design and Synthesis. crRNA sequences (20 bp) for each gene were inserted behind the T7 promoter sequence (5′-GAAATTAATACGACTCACTATAGGN20GTTTT AGAGCTAGAAATAGCAAGT TAAAATAAGGCTAGTCCG-3′). The reverse template sequence (5′-AAAAAAGCACCGACTCGGTGCCACTTTTTCAAGTTGATAACGGAC TAGCCTTATTTTAACTTGC-3′) was used to synthesize the dsDNA template using Power-Pfu (500 U/μL, NanoHelix) and dNTPs (10 mM, Thermo Scientific). *In vitro* transcription was performed by mixing dsDNA template, T7 RNA polymerase (50,000 units/mL, New England Biolabs), 50 mM $MgCl_2$, 0.1 M DTT, rNTPs (100 mM, Jena Bioscience), and RNase inhibitor murine (40,000 units/mL, New England Biolabs) at 37 °C for 16 h. Then, the synthesized sgRNA was precipitated with isopropanol (Sigma) and purified with a GeneAll ExpinTM PCR SV kit (GeneAll Biotechnology). Purified sgRNA concentration was measured using a NanoDrop 2000 (Thermo Scientific). Purity of the fully synthesized sgRNA was checked by running 1.0% denaturing formaldehyde gels with a MOPS buffer (Biosolution).

Functional Analyses of dCas9/sgRNA Complexes. To examine DNA cleavage, 1 μg of purified Cas9 protein and 750 ng of sgRNA were mixed with 120 ng of amplified target DNA in NEB3.1 buffer (25 mM Tris-HCl, 50 mM NaCl, 5 mM $MgCl_2$, and 50 μg/mL BSA, New England Biolabs). The mixture was reacted at 37 °C for 90 min using SimpliAmp Thermal Cycler (Applied Biosystems). After the reaction, cleaved DNA was purified with GeneAll ExpinTM PCR SV kit (GeneAll Biotechnology) and analyzed by 1.0% agarose gel electrophoresis. To determine target

https://doi.org/10.1021/acsami.3c17151
ACS Appl. Mater. Interfaces 2024, 16, 5637−5647

DNA binding, 100 ng of dCas9 protein, 100 ng of sgRNA, and 50 ng of amplified target DNA were mixed in NEB 3.1 buffer. The mixture was reacted at conditions used for the DNA cleavage assay and analyzed by 8.0% polyacrylamide gel electrophoresis (PAGE).

Bacterial Culture. The bacterial strains *E. coli* (#1682), *P. aeruginosa* (#2450), and *S. aureus* (#3881) were obtained from the Korean Collection for Type Cultured (KCTC). Methicillin-resistant *S. aureus* (MRSA, #3877) was obtained from the Culture Collection of Antimicrobial Resistant Microbes (CCARM). Carbapenem-resistant *K. pneumoniae* (CRKP) and *NDM-1* (+) *E. coli* were isolated from Asan Medical Center (Seoul, Korea). All bacteria were cultured in LB medium until OD_{600} = 0.8−1.0.

Amplification of Target Nucleic Acids. RT-LAMP was performed by reaction of 10 ng of bacterial total RNA in 1× isothermal amplification buffer (New England Biolabs), added with Bst 2.0 WarmStart DNA Polymerase (8000 U/mL, New England Biolabs), WarmStart RTx Reverse Transcriptase (15,000 U/mL, New England Biolabs), and dNTPs (10 mM, Thermo Scientific), 1.6 μM each of FIP and BIP, 0.2 μM each of F3 and B3 (Table S2). The reaction was performed using SimpliAmp Thermal Cycler (Applied Biosystems) with the following conditions: 65 °C for 30 min and 80 °C for 5 min. The amplified product was analyzed by 1.0% agarose gel electrophoresis with a TBE buffer.

Electrochemical Sensing using Sourcemeter and EIS. To determine the performance of electrochemical sensing, the dCas9-PD-Cu-coated Si wafer was treated with 62.5 nM sgRNA(*mecA*) or sgRNA(*kpc-2*) for 1 h at room temperature. After washing with PBS pH 7.4 and drying, the dCas9-PD-Cu/sgRNA(*mecA*) or dCas9-PD-Cu/sgRNA(*kpc-2*) electrode was used to detect *mecA* or *kpc-2* target DNA. The electrochemical sensing of target DNA was based on the change in resistance of the electrodes by binding of the target DNA with sgRNA on the electrode surface. The as-modified electrode was incubated in *mecA* or *kpc-2* target DNA solution for 1 h at room temperature. After taking out from the solution, the electrode was washed with PBS pH 7.4 and dried prior to the measurement. The change in resistance of the electrode was measured by using a two-electrode system of sourcemeter (DC resistance measurement) and EIS (frequency range: 10^4−10^0 Hz, −1.2 V vs OCP), with the equivalent circuit (simple Randle circuit) illustrated in Figure S16.

Wireless Sensing. A wireless sensing platform was designed based on the 2-electrode DC resistance measurement system that consisted of a Bluetooth module (AppGosu), a microcontroller unit (Arduino Uno), and a smartphone.[45] The wireless platform was calibrated using 1 to 20 MΩ standard resistors based on the obtained sample resistance (via sourcemeter). The coated surface was connected to a microcontroller and a Bluetooth module using alligator clips. While sensing, the measured resistance value was transmitted and displayed to a smartphone as a resistance graph by activating the Bluetooth connection.

Quantitative Real-Time PCR (qPCR). Bacterial total RNA was extracted using TRIzol (Life Technologies) according to the manufacturer's protocol. RNA quality was confirmed by measuring A260/A280 and A260/A230 ratios using a NanoDrop 2000 instrument (Thermo Scientific). cDNA synthesis was performed with a PrimeScript RT reagent kit (Takara) using SimpliAmp Thermal Cycler (Applied Biosystems). To generate a standard curve for absolute quantification, DNA from each target gene was amplified using primers (Table S3). Quantification of gene expression was carried out with PowerUp SYBR Green Master Mix (Applied Biosystems) and primers (Table S4) using QuantSudio 3 Real-Time PCR system (Applied Biosystems) with conditions as follows: 1 cycle of 95 °C for 2 min, followed by 50 cycles of 95 °C for 15 s, 60 °C for 15 s, and 72 °C for 1 min. Melting curve analysis was performed by increasing the reaction temperature from 60 to 95 °C at a rate of 0.15 °C/s.

Diagnosis of Clinical Samples. Human sputum specimens were randomly obtained from patients who were diagnosed with bacterial pneumonia at Asan Medical Center (IRB no.: 2021-0298). The sputum samples were diluted with PBS, and the dispersible phase was centrifuged (8500*g*, 15 min), followed by total RNA extraction, reverse transcription, and amplification as described above. The amplified samples were applied to the dCas9-PD-Cu sensor for diagnosis. Microbial culture results were obtained from the clinical microbiology laboratory at the Asan Medical Center.

■ ASSOCIATED CONTENT

Supporting Information

The Supporting Information is available free of charge at https://pubs.acs.org/doi/10.1021/acsami.3c17151.

Physical characterization of synthesized PD and PD-Cu (Figure S1), characterization of PD and PD-Cu coated on PET substrate (Figure S2), purification of dCas9 (Figure S3), synthesis of sgRNA (Figure S4), specificity of sgRNAs targeting *mecA* and *kpc-2* (Figure S5), specificity of sgRNAs targeting *NDM-1* and *ClfA* (Figure S6), binding specificity of sgRNAs with dCas9 to target DNAs (Figure S7), sourcemeter measurements of dCas9-PD-Cu when complexed with sgRNA (Figure S8), characterization of LAMP products from various bacterial strains (Figure S9), characterization of LAMP products according to various incubation times (Figure S10), qPCR for *NDM-1* gene in various bacterial strains (Figure S11), wireless sensing of patients' samples using dCas9-PD-Cu targeting *mecA* gene (Figure S12), qPCR of patients' samples for *mecA* and *kpc-2* genes (Figure S13), oligonucleotide templates for sgRNA synthesis (Table S1), primers for LAMP (Table S2), qPCR primers for absolute quantification of target RNAs (Table S3), and primers for qPCR (Table S4) (PDF)

■ AUTHOR INFORMATION

Corresponding Authors

Yang Soo Kim − *Division of Infectious Diseases, Asan Medical Center, University of Ulsan College of Medicine, Seoul 05505, Republic of Korea*; Email: yskim@amc.seoul.kr

Sung Young Park − *Department of Chemical and Biological Engineering, Korea National University of Transportation, Chungju 380-702, Republic of Korea; Department of Green Bio Engineering and Department of IT and Energy Convergence, Korea National University of Transportation, Chungju 380-702, Republic of Korea;* orcid.org/0000-0002-0358-6946; Email: parkchem@ut.ac.kr

Hyun Jung Chung − *Department of Biological Sciences, Korea Advanced Institute of Science and Technology, Daejeon 34141, Republic of Korea;* orcid.org/0000-0001-5055-902X; Email: hyunjc@kaist.ac.kr

Authors

San Hae Im − *Department of Biological Sciences, Korea Advanced Institute of Science and Technology, Daejeon 34141, Republic of Korea*

Akhmad Irhas Robby − *Department of Chemical and Biological Engineering, Korea National University of Transportation, Chungju 380-702, Republic of Korea*

Heewon Choi − *Department of Biological Sciences, Korea Advanced Institute of Science and Technology, Daejeon 34141, Republic of Korea*

Ju Yeon Chung − *Department of Biological Sciences, Korea Advanced Institute of Science and Technology, Daejeon 34141, Republic of Korea*

Complete contact information is available at: https://pubs.acs.org/10.1021/acsami.3c17151

https://doi.org/10.1021/acsami.3c17151
ACS Appl. Mater. Interfaces 2024, 16, 5637−5647

Author Contributions

#S.H.I. and A.I.R. have contributed equally to this work. S.H.I., A.I.R., Y.S.K., S.Y.P., and H.J.C. designed the project. H.C. and J.Y.C. contributed to the process of clinical samples. All authors have contributed to the analysis and interpretation of the data and writing the manuscript.

Notes

The authors declare no competing financial interest.

■ ACKNOWLEDGMENTS

This work was supported by the Korea Medical Device Development Fund (no. 202011D08/RS-2020-KD000071), the National Research Foundation of Korea (nos. 2021R1A2C2011763, 2021M3E5E3080383, and 2018R1A6A1A03023788), and the Ministry of Health and Welfare (no. HI22C2010).

■ REFERENCES

(1) G. B. D. Antimicrobial Resistance Collaborators; Ikuta, K. S.; Swetschinski, L. R.; Aguilar, G. R.; Sharara, F.; Mestrovic, T.; Gray, A. P.; Weaver, N. D.; Wool, E. E.; Han, C.; Hayoon, A. G. Global Mortality Associated with 33 Bacterial Pathogens in 2019: A Systematic Analysis for the Global Burden of Disease Study 2019. *Lancet* **2023**, *400* (10369), 2221−2248.

(2) Ryan, D.; Ojha, U. K.; Jaiswal, S.; Padhi, C.; Suar, M. The Small RNA DsrA Influences the Acid Tolerance Response and Virulence of *Salmonella Enterica* Serovar Typhimurium. *Front. Microbiol.* **2016**, *7*, 599.

(3) Pati, N. B.; Vishwakarma, V.; Jaiswal, S.; Periaswamy, B.; Hardt, W.-D.; Suar, M. Deletion of InvH Gene in *Salmonella Enterica* Serovar Typhimurium Limits the Secretion of Sip Effector Proteins. *Microbes Infect.* **2013**, *15* (1), 66−73.

(4) May, M. Tomorrow's Biggest Microbial Threats. *Nat. Med.* **2021**, *27* (3), 358−359.

(5) O'neill, J. *Antimicrobial Resistance: Tackling a Crisis for the Health and Wealth of Nations*; Review on Antimicrobial Resistance, 2014.

(6) Baker, C. N.; Stocker, S. A.; Culver, D. H.; Thornsberry, C. Comparison of the E Test to Agar Dilution, Broth Microdilution, and Agar Diffusion Susceptibility Testing Techniques by Using a Special Challenge Set of Bacteria. *J. Clin. Microbiol.* **1991**, *29* (3), 533−538.

(7) Wareham, D. W.; Shah, R.; Betts, J. W.; Phee, L. M.; Momin, M. H. F. A. Evaluation of an Immunochromatographic Lateral Flow Assay (OXA-48 K -SeT) for Rapid Detection of OXA-48-Like Carbapenemases in *Enterobacteriaceae*. *J. Clin. Microbiol.* **2016**, *54* (2), 471−473.

(8) Tada, T.; Sekiguchi, J.-I.; Watanabe, S.; Kuwahara-Arai, K.; Mizutani, N.; Yanagisawa, I.; Hishinuma, T.; Zan, K. N.; Mya, S.; Tin, H. H.; Kirikae, T. Assessment of a Newly Developed Immunochromatographic Assay for NDM-Type Metallo-β-Lactamase Producing Gram-Negative Pathogens in Myanmar. *BMC Infect. Dis.* **2019**, *19* (1), 565.

(9) Amini, M.; Pourmand, M. R.; Faridi-Majidi, R.; Heiat, M.; Nezhady, M. A. M.; Safari, M.; Noorbakhsh, F.; Baharifar, H. Optimising Effective Parameters to Improve Performance Quality in Lateral Flow Immunoassay for Detection of PBP2a in Methicillin-Resistant *Staphylococcus Aureus* (MRSA). *J. Exp. Nanosci.* **2020**, *15* (1), 266−279.

(10) Yamada, K.; Wanchun, J.; Ohkura, T.; Murai, A.; Hayakawa, R.; Kinoshita, K.; Mizutani, M.; Okamoto, A.; Namikawa, T.; Ohta, M. Detection of Methicillin-Resistant *Staphylococcus Aureus* Using a Specific Anti-PBP2a Chicken IgY Antibody. *Jpn. J. Infect. Dis.* **2013**, *66* (2), 103−108.

(11) Chen, G.; Abdeen, A. A.; Wang, Y.; Shahi, P. K.; Robertson, S.; Xie, R.; Suzuki, M.; Pattnaik, B. R.; Saha, K.; Gong, S. A Biodegradable Nanocapsule Delivers a Cas9 Ribonucleoprotein Complex for in Vivo Genome Editing. *Nat. Nanotechnol.* **2019**, *14* (10), 974−980.

(12) Wei, T.; Cheng, Q.; Min, Y.-L.; Olson, E. N.; Siegwart, D. J. Systemic Nanoparticle Delivery of CRISPR-Cas9 Ribonucleoproteins for Effective Tissue Specific Genome Editing. *Nat. Commun.* **2020**, *11* (1), 3232.

(13) Cheng, Q.; Wei, T.; Farbiak, L.; Johnson, L. T.; Dilliard, S. A.; Siegwart, D. J. Selective Organ Targeting (SORT) Nanoparticles for Tissue-Specific MRNA Delivery and CRISPR−Cas Gene Editing. *Nat. Nanotechnol.* **2020**, *15* (4), 313−320.

(14) Deveau, H.; Garneau, J. E.; Moineau, S. CRISPR/Cas System and Its Role in Phage-Bacteria Interactions. *Annu. Rev. Microbiol.* **2010**, *64* (1), 475−493.

(15) Horvath, P.; Barrangou, R. CRISPR/Cas, the Immune System of Bacteria and Archaea. *Science* **2010**, *327* (5962), 167−170.

(16) Zhuang, J.; Zhao, Z.; Lian, K.; Yin, L.; Wang, J.; Man, S.; Liu, G.; Ma, L. SERS-Based CRISPR/Cas Assay on Microfluidic Paper Analytical Devices for Supersensitive Detection of Pathogenic Bacteria in Foods. *Biosens. Bioelectron.* **2022**, *207*, 114167.

(17) Li, Y.; Liao, D.; Kou, J.; Tong, Y.; Daniels, L. C.; Man, S.; Ma, L. Comparison of CRISPR/Cas and Argonaute for Nucleic Acid Tests. *Trends Biotechnol.* **2023**, *41* (5), 595−599.

(18) Li, Y.; Zhao, Z.; Liu, Y.; Wang, N.; Man, S.; Ma, L.; Wang, S. CRISPR/Cas System: The Accelerator for the Development of Non-Nucleic Acid Target Detection in Food Safety. *J. Agric. Food Chem.* **2023**, *71* (37), 13577−13594.

(19) Ma, L.; Zhang, W.; Yin, L.; Li, Y.; Zhuang, J.; Shen, L.; Man, S. A SERS-Signalled, CRISPR/Cas-Powered Bioassay for Amplification-Free and Anti-Interference Detection of SARS-CoV-2 in Foods and Environmental Samples Using a Single Tube-in-Tube Vessel. *J. Hazard. Mater.* **2023**, *452*, 131195.

(20) Bhattacharjee, R.; Nandi, A.; Mitra, P.; Saha, K.; Patel, P.; Jha, E.; Panda, P. K.; Singh, S. K.; Dutt, A.; Mishra, Y. K.; Verma, S. K.; Suar, M. Theragnostic Application of Nanoparticle and CRISPR against Food-Borne Multi-Drug Resistant Pathogens. *Mater. Today Bio* **2022**, *15*, 100291.

(21) Chen, J. S.; Ma, E.; Harrington, L. B.; Costa, M. D.; Tian, X.; Palefsky, J. M.; Doudna, J. A. CRISPR-Cas12a Target Binding Unleashes Indiscriminate Single-Stranded DNase Activity. *Science* **2018**, *360* (6387), 436−439.

(22) Gootenberg, J. S.; Abudayyeh, O. O.; Kellner, M. J.; Joung, J.; Collins, J. J.; Zhang, F. Multiplexed and Portable Nucleic Acid Detection Platform with Cas13, Cas12a, and Csm6. *Science* **2018**, *360* (6387), 439−444.

(23) Gootenberg, J. S.; Abudayyeh, O. O.; Lee, J. W.; Essletzbichler, P.; Dy, A. J.; Joung, J.; Verdine, V.; Donghia, N.; Daringer, N. M.; Freije, C. A.; Myhrvold, C.; Bhattacharyya, R. P.; Livny, J.; Regev, A.; Koonin, E. V.; Hung, D. T.; Sabeti, P. C.; Collins, J. J.; Zhang, F. Nucleic Acid Detection with CRISPR-Cas13a/C2c2. *Science* **2017**, *356* (6336), 438−442.

(24) Jinek, M.; Chylinski, K.; Fonfara, I.; Hauer, M.; Doudna, J. A.; Charpentier, E. A Programmable Dual-RNA−Guided DNA Endonuclease in Adaptive Bacterial Immunity. *Science* **2012**, *337* (6096), 816−821.

(25) Tanenbaum, M. E.; Gilbert, L. A.; Qi, L. S.; Weissman, J. S.; Vale, R. D. A Protein-Tagging System for Signal Amplification in Gene Expression and Fluorescence Imaging. *Cell* **2014**, *159* (3), 635−646.

(26) Jiang, W.; Aman, R.; Ali, Z.; Mahfouz, M. Bio-SCAN V2: A CRISPR/DCas9-Based Lateral Flow Assay for Rapid Detection of Theophylline. *Front. Bioeng. Biotechnol.* **2023**, *11*, 1118684.

(27) Qiu, X.-Y.; Zhu, L.-Y.; Zhu, C.-S.; Ma, J.-X.; Hou, T.; Wu, X.-M.; Xie, S.-S.; Min, L.; Tan, D.-A.; Zhang, D.-Y.; Zhu, L. Highly Effective and Low-Cost MicroRNA Detection with CRISPR-Cas9. *ACS Synth. Biol.* **2018**, *7* (3), 807−813.

(28) Bengtson, M.; Bharadwaj, M.; Franch, O.; van der Torre, J.; Meerdink, V.; Schallig, H.; Dekker, C. CRISPR-DCas9 Based DNA Detection Scheme for Diagnostics in Resource-Limited Settings. *Nanoscale* **2022**, *14* (5), 1885−1895.

(29) Zhang, Y.; Qian, L.; Wei, W.; Wang, Y.; Wang, B.; Lin, P.; Liu, W.; Xu, L.; Li, X.; Liu, D.; Cheng, S.; Li, J.; Ye, Y.; Li, H.; Zhang, X.;

https://doi.org/10.1021/acsami.3c17151
ACS Appl. Mater. Interfaces 2024, 16, 5637−5647

Dong, Y.; Zhao, X.; Liu, C.; Zhang, H. M.; Ouyang, Q.; Lou, C. Paired Design of DCas9 as a Systematic Platform for the Detection of Featured Nucleic Acid Sequences in Pathogenic Strains. *ACS Synth. Biol.* **2017**, *6* (2), 211−216.
(30) Li, Y.; Qiao, J.; Zhao, Z.; Zhang, Q.; Zhang, W.; Man, S.; Ye, S.; Chen, K.; Ma, L. A CRISPR/DCas9-enabled, On-site, Visual, and Bimodal Biosensing Strategy for Ultrasensitive and Self-validating Detection of Foodborne Pathogenic Bacteria. *Food Front.* **2023**, *4*, 2070−2080.
(31) Jo, H. J.; Robby, A. I.; Kim, S. G.; Lee, G.; Lee, B. C.; Park, S. Y. Reusable Biosensor-Based Polymer Dot-Coated Electrode Surface for Wireless Detection of Bacterial Contamination. *Sens. Actuators, B* **2021**, *346*, 130503.
(32) Güney, S. An Electrochemical Sensor Based on Molecularly Imprinted Polydopamine Coated on Reduced Graphene Oxide for Selective Detection of Ornidazole. *Electroanalysis* **2023**, *35* (7), No. e202200477.
(33) Linh, N. D.; Huyen, N. T. T.; Dang, N. H.; Piro, B.; Thu, V. T. Electrochemical Interface Based on Polydopamine and Gold Nanoparticles/Reduced Graphene Oxide for Impedimetric Detection of Lung Cancer Cells. *RSC Adv.* **2023**, *13* (15), 10082−10089.
(34) Wei, J.; Wu, C.; Wu, X.; Wu, L. A Sensitive Electrochemical Bisphenol A Sensor Based on Molecularly Imprinted Polydopamine-Coated Fe_3O_4 Microspheres. *Anal. Sci.* **2021**, *38* (2), 21P278.
(35) Swamy, N. K.; Mohana, K. N. S.; Hegde, M. B.; Madhusudana, A. M.; Rajitha, K.; Nayak, S. R. Fabrication of Graphene Nanoribbon-Based Enzyme-Free Electrochemical Sensor for the Sensitive and Selective Analysis of Rutin in Tablets. *J. Appl. Electrochem.* **2021**, *51* (7), 1047−1057.
(36) Hegde, M. B.; Mohana, K. N. S.; Madhusudhana, A. M.; Vinay, M. M.; Nayaka, Y. A.; Swamy, N. K. Fabrication of Reduced Graphene Oxide/Ruthenium Oxide Modified Graphite Electrode for Voltammetric Determination of Tryptophan. *Graphene 2D Mater. Technol.* **2021**, *6* (3−4), 25−34.
(37) Qian, L.; Thiruppathi, A. R.; van der Zalm, J.; Chen, A. Graphene Oxide-Based Nanomaterials for the Electrochemical Sensing of Isoniazid. *ACS Appl. Nano Mater.* **2021**, *4* (4), 3696−3706.
(38) Wu, Y.; Shi, C.; Wang, G.; Sun, H.; Yin, S. Recent Advances in the Development and Applications of Conjugated Polymer Dots. *J. Mater. Chem. B* **2022**, *10* (16), 2995−3015.
(39) Jo, H. J.; Ryu, J. S.; Robby, A. I.; Kim, Y. S.; Chung, H. J.; Park, S. Y. Rapid and Selective Electrochemical Sensing of Bacterial Pneumonia in Human Sputum Based on Conductive Polymer Dot Electrodes. *Sens. Actuators, B* **2022**, *368*, 132084.
(40) Kim, S. G.; Ryplida, B.; Giang, N. N.; Lee, G.; Lee, K. D.; Park, S. Y. Tuning Conductivity and Roughness of Diselenide Polymer Dot-Coated Surface for ROS-Mediated Selective Real-Time Wireless Detection of Cancer Cells. *Chem. Eng. J.* **2021**, *426*, 130880.
(41) Zhang, Q.; Guo, Z.; Zheng, X. Synthesis of Ag@carbonized Polymer Dots and Their Electrochemical Sensing of MiRNA. *Electroanalysis* **2023**, *35* (2), No. e202200190.
(42) Kim, S. G.; Robby, A. I.; Kim, E. H.; Jin, E.-J.; Park, S. Y. Pyrophosphate-Responsive Viscoelasticity and Conductive Signaling of Self-Reporting Hydrogel Sensor for Detection of Cancer Cells. *Chem. Eng. J.* **2023**, *472*, 145069.
(43) Sinha, A.; Bhattacharjee, R.; Bhattacharya, B.; Nandi, A.; Shekhar, R.; Jana, A.; Saha, K.; Kumar, L.; Patro, S.; Panda, P. K.; Kaushik, N. K.; Suar, M.; Verma, S. K. The Paradigm of MiRNA and SiRNA Influence in Oral-Biome. *Biomed. Pharmacother.* **2023**, *159*, 114269.
(44) Notomi, T.; Okayama, H.; Masubuchi, H.; Yonekawa, T.; Watanabe, K.; Amino, N.; Hase, T. Loop-Mediated Isothermal Amplification of DNA. *Nucleic Acids Res.* **2000**, *28* (12), No. e63.
(45) Jo, H. J.; Yang, J.-H.; Robby, A. I.; Lee, G.; Jin, E.-J.; Park, S. Y. Cancer Microenvironment-Recognizable Negative−Positive Electronic Signal-Based Pore Size-Tunable PH/ROS-Responsive Hydrogel Sensor. *Sens. Actuators, B* **2023**, *390*, 133945.

https://doi.org/10.1021/acsami.3c17151
ACS Appl. Mater. Interfaces 2024, 16, 5637−5647